1521-0103/365/3/544–555$35.00
THE JOURNAL OF PHARMACOLOGY AND EXPERIMENTAL THERAPEUTICS

https://doi.org/10.1124/jpet.117.247320
J Pharmacol Exp Ther 365:544–555, June 2018

The Journal of PHARMACOLOGY And Experimental Therapeutics

Transient Receptor Potential Melastatin-8 Activation Induces Relaxation of Pulmonary Artery by Inhibition of Store-Operated Calcium Entry in Normoxic and Chronic Hypoxic Pulmonary Hypertensive Rats

Yun-Ping Mu,[1] Da-Cen Lin,[1] Si-Yi Zheng,[1] Hai-Xia Jiao, James S. K. Sham, and Mo-Jun Lin

Key Laboratory of Fujian Province Universities on Ion Channel and Signal Transduction in Cardiovascular Diseases (Y.-P.M., D.-C.L., S.-Y.Z., H.-X.J., J.S.K.S., M.-J.L.) and Department of Physiology and Pathophysiology (Y.-P.M., D.-C.L., S.-Y.Z., H.-X.J., M.-J.L.), School of Basic Medical Sciences, Fujian Medical University, Fuzhou, Fujian Province, People's Republic of China; and Division of Pulmonary and Critical Care Medicine, Johns Hopkins University School of Medicine, Baltimore, Maryland (Y.-P.M., J.S.K.S.)

Received December 20, 2017; accepted April 4, 2018

ABSTRACT

Pulmonary hypertension (PH) is characterized by enhanced vasoconstriction and vascular remodeling, which are attributable to the alteration of Ca^{2+} homeostasis in pulmonary arterial smooth muscle cells (PASMCs). It is well established that store-operated Ca^{2+} entry (SOCE) is augmented in PASMCs during PH and that it plays a crucial role in PH development. Our previous studies showed that the melastatin-related transient receptor potential 8 (TRPM8) is down-regulated in PASMCs of PH animal models, and activation of TRPM8 causes relaxation of pulmonary arteries (PAs). However, the mechanism of TRPM8-induced PA relaxation is unclear. Here we examined the interaction of TRPM8 and SOCE in PAs and PASMCs of normoxic and chronic hypoxic pulmonary hypertensive (CHPH) rats, a model of human group 3 PH. We found that TRPM8 was down-regulated and TRPM8-mediated cation entry was reduced in CHPH-PASMCs. Activation of TRPM8 with icilin caused concentration-dependent relaxation of cyclopiazonic acid (CPA) and endothelin-1 contracted endothelium-denuded PAs, and the effect was abolished by the SOCE antagonist Gd^{3+}. Application of icilin to PASMCs suppressed CPA-induced Mn^{2+} quenching and Ca^{2+} entry, which was reversed by the TRPM8 antagonist *N*-(3-aminopropyl)-2-([(3-methylphenyl)methyl])-oxy-*N*-(2-thienylmethyl)benzamide hydrochloride salt (AMTB). Moreover, the inhibitory effects of icilin on SOCE in PA and PASMCs of CHPH rats were significantly augmented due to enhanced SOCE activity in PH. Our results, therefore, demonstrated a novel mechanism of TRPM8-mediated inhibition of SOCE in pulmonary vasculature. Because SOCE is important for vascular remodeling and enhanced vasoconstriction, down-regulation of TRPM8 in PASMCs of CHPH rats may minimize its inhibitory influence to allow unimpeded SOCE activity for PH development.

Introduction

Pulmonary hypertension (PH) is a pathologic condition associated with a wide spectrum of diseases. It is classified into five categories: pulmonary arterial hypertension (PAH) (group 1); PH due to left heart disease (group 2); PH due to lung diseases and/or hypoxia (group 3); chronic thromboembolic PH (group 4); and PH with unclear multifactorial mechanisms (group 5) (Simonneau et al., 2013). Many forms of PH exhibit progressive increase in pulmonary vascular resistance due to sustained pulmonary vasoconstriction and vascular remodeling; in the case of severe PH, such as PAH, this leads to right heart failure and death (Stenmark et al., 2006; Lai et al., 2014). The cellular and molecular mechanisms of PH are complex, but the disturbance of Ca^{2+} homeostasis within pulmonary arterial smooth muscle cells (PASMCs) is recognized as an important trigger for the pathogenesis of PH (Remillard and Yuan, 2006). In vascular smooth muscle cells (VSMCs), the transient receptor potential

This work was supported by grants from the National Natural Science Foundation of China [NSFC31571179 and NSFC31371165], Natural Science Foundation of Fujian Province [2015J01313] and the Fujian Province Hundred Experts Award.
[1]Y.-P.M., D.-C.L., and S.-Y. Z contributed equally to this work.
https://doi.org/10.1124/jpet.117.247320.

ABBREVIATIONS: AMTB, *N*-(3-aminopropyl)-2-([(3-methylphenyl)methyl])-oxy-*N*-(2-thienylmethyl)benzamide hydrochloride salt; CH, chronic hypoxia; CHPH, chronic hypoxic pulmonary hypertension; CPA, cyclopiazonic acid; ER, endoplasmic reticulum; ET-1, endothelin-1; HBSS, Hanks' balanced salt solution; IPAH, idiopathic pulmonary arterial hypertension; LV, left ventricle; PA, pulmonary artery; PASMC, pulmonary arterial smooth muscle cell; PBS, phosphate-buffered saline; PH, pulmonary hypertension; P_{Pa}, pulmonary arterial pressure; ROS, reactive oxygen species; RV, right ventricle; RVMI, right ventricular mass index; RVSP, right ventricle systolic pressure; S, septum; SOCE, store-operated Ca^{2+} entry; SR, sarcoplasmic reticulum; STIM, stromal interaction molecule; TRP, transient receptor potential; TRPC, canonical transient receptor potential; TRPM8, transient receptor potential melastatin-8; U46619, 9,11-dideoxy-9α,11α-methanoepoxy prostaglandin F2α; VDCC, voltage-gated Ca^{2+} channels; VSMC, vascular smooth muscle cell.

(TRP) superfamily encodes a large repertoire of cation channels, which play critical roles in many vascular functions including myogenic response, agonist-induced vasoconstriction, and VSMC proliferation (Inoue et al., 2006). Growing evidence suggests that several members of TRP subfamilies are involved in PH development (Lin et al., 2004; Yang et al., 2012; Liu et al., 2013; Xia et al., 2013, 2014).

The canonical TRP (TRPC) channels regulate vascular function mainly by modulating $[Ca^{2+}]_i$ through store-operated Ca^{2+} entry (SOCE) and receptor-operated Ca^{2+} entry (Lin et al., 2004; Remillard and Yuan, 2006). SOCE is the best recognized Ca^{2+} entry pathway for playing a critical role in PH (Lin et al., 2004; Yu et al., 2004; Morrell et al., 2009; Fernandez et al., 2012; Kuhr et al., 2012). It is activated subsequent to Ca^{2+} release from endoplasmic/sarcoplasmic reticulum (ER/SR) (Putney, 2009). The decrease in SR Ca^{2+} level is detected by the Ca^{2+} sensors stromal interaction molecules (STIM1 or STIM2) (Roos et al., 2005; Zhang et al., 2005), which oligomerize and translocate to the SR-plasma membrane junctions and couple with the store-operated cation channels (e.g., Orai1, Orai2, TRPC) to mediate Ca^{2+} entry (Soboloff et al., 2012; Choi et al., 2014).

In PASMCs, TRPC1 and Orai1 are the major channels for SOCE. Small interfering RNA (siRNA) knockdown of these proteins inhibits SOCE (Sweeney et al., 2002; Lin et al., 2004, 2016; Ng et al., 2012); and overexpression of TRPC1 enhances SOCE (Kunichika et al., 2004). Other TRPC channels such as TRPC6 could be involved in SOCE during PASMC proliferation (Yu et al., 2003, 2004; Zhang et al., 2004a). Previous studies consistently showed that enhanced SOCE are associated with TRPC1 up-regulation in PASMCs of chronic hypoxia (CH) and monocrotaline-induced PH animal models (Lin et al., 2004; Liu et al., 2012; Xia et al., 2014) and TRPC6 up-regulation in PASMCs of idiopathic pulmonary arterial hypertension (IPAH) patients (Yu et al., 2004; Zhang et al., 2007; Song et al., 2011; Fernandez et al., 2015). Deletion of *trpc1* and/or *trpc6* genes can effectively attenuate chronic hypoxic pulmonary hypertension (CHPH) in mice (Malczyk et al., 2013; Xia et al., 2014; Smith et al., 2015). Moreover, a functional single nucleotide polymorphism of TRPC6 has been identified in patients of IPAH (Yu et al., 2009). These findings clearly suggest that TRPC1- and TRPC6-mediated SOCE are important signaling pathways related to the development of PH.

In contrast to the TRPC channels, the role of melastatin-related TRPM channels in pulmonary vascular function and PH is more obscure. We previously showed that several TRPM channel subtypes are expressed in rat pulmonary arteries (PAs) and aorta, with TRPM8 being the most abundant TRPM subtype (Yang et al., 2006). Activation of TRPM8 with menthol induced an increase in $[Ca^{2+}]_i$ that could be abolished by the removal of extracellular Ca^{2+} or application of Ni^{2+}, indicating that TRPM8 is a functional channel in PASMCs. TRPM8 agonists have minimal effect on the relaxed PAs but caused significant vasorelaxation after agonist-induced contraction in endothelium-denuded PAs (Liu et al., 2013). More importantly, TRPM8 channel is the only member of the TRP channels that is down-regulated in PAs of CH and monocrotaline-induced PH rats (Yang et al., 2012; Liu et al., 2013). The down-regulation occurs in the early stage of PH and persists throughout PH development (Liu et al., 2013), suggesting that the process may be related to PH pathogenesis. However, the precise physiologic functions of TRPM8 in the pulmonary vasculature and its role in PH are unclear.

TRPM8 was originally identified as a prostate-specific gene in human prostate carcinoma cells (Tsavaler et al., 2001) and a cold-sensitive ion channel in sensory neurons (Peier et al., 2002). It is localized in both the plasma membrane and SR to mediate extracellular cation influx and intracellular Ca^{2+} release, respectively (Bidaux et al., 2007; Melanaphy et al., 2016; Xiong et al., 2017). In systemic VSMCs, TRPM8-mediated SR Ca^{2+} release regulates mitochondrial reactive oxygen species (ROS) generation to antagonize vasoconstriction and hypertension through inhibition of the RhoA/Rho kinase pathway (Sun et al., 2014; Xiong et al., 2017). It has been shown in the prostate cancer-derived epithelial cells that stimulation of TRPM8 causes Ca^{2+} release from ER and activates SOCE (Thebault et al., 2005). However, the participation of TRPM8 in SOCE has not been determined in VSMCs.

In view of the importance of SOCE in PH, we hypothesize that TRPM8 and SOCE interact functionally and contribute to the altered pulmonary vascular function in PH. In this study, we used the CHPH rat model, a close resemblance of the human group 3 PH, to examine the possible interactions of TRPM8 and SOCE in PAs under normal physiologic conditions and pathologic conditions during the development of PH.

Methods

Animal Model of CH-Induced PH. Male Sprague-Dawley rats (200–220 g) obtained from the animal center of Fujian Medical University were placed in a hypoxic chamber (9.5%–10.5% O_2) for 3 weeks as described previously elsewhere (Lin et al., 2004; Liu et al., 2013). They were housed under controlled temperature conditions (24°C) with food and water given ad libitum. At the end of CH exposure, animals were anesthetized with urethane (1 g/kg), and ventilated with a volume-controlled ventilator (Inspira ASC; Harvard Apparatus, Cambridge, MA). Right ventricle systolic pressure (RVSP) and pulmonary arterial pressure (P_{Pa}) were measured using a Mikro-Tip pressure catheter (Millar Instruments, Houston, TX) through direct puncture of the right ventricle (RV), followed by advancing the catheter into the main PA, using an open-chest approach. At the end of hemodynamic measurement, the heart and lungs were dissected. Right ventricular mass index (RVMI) was determined by the mass ratio of RV to left ventricle (LV) plus septum (S)[RV/(LV + S)] as an index of RV hypertrophy. All animal protocols were approved by the Animal Care and Use Committee of Fujian Medical University in accordance to the national guidelines.

Isometric Contraction of Intralobar PAs. Intralobar PAs (300~800 μm o.d.) were isolated in oxygenated modified Krebs' solution containing 118 mM NaCl, 4.7 mM KCl, 1.2 mM $MgCl_2$, 10 mM HEPES, 11.1 mM glucose, and 2.0 mM $CaCl_2$, and cut into 4-mm length rings. The endothelium of PA was disrupted by gently rubbing the inner intimal surface with a small wooden stick (Liu et al., 2013; Jiao et al., 2016). PA rings were suspended in organ chambers filled with modified Krebs' solution aerated with 95% O_2 plus 5% CO_2, and isometric contraction was measured with force transducers (Chengdu Instrument Factory, Chengdu, People's Republic of China). Resting tension was adjusted to 0.8~1 g. After 1 hour of equilibration, arterial rings were exposed 3 times to KCl (60 mM) to establish maximum contraction, and then to phenylephrine (3 μM) followed by acetylcholine (10 μM) to verify the complete disruption of endothelium. Arterial rings with >20% acetylcholine-induced relaxation were discarded.

Isolation and Culture of PASMCs. PASMCs were isolation enzymatically and transiently cultured as previously described elsewhere (Liu et al., 2013; Jiao et al., 2016). Briefly, the lungs were removed and transferred to a Petri dish filled with cold HEPES-buffered salt solution containing 130 mM NaCl, 5 mM KCl, 1.2 mM $MgCl_2$, 10 mM HEPES, 10 mM glucose, and 1.5 mM $CaCl_2$. The third- and fourth-generation PAs were isolated and cleaned free of connective tissue. Endothelium was removed by gently rubbing the luminal surface with a cotton swab. The arteries were then allowed to recover for 30 minutes in cold (4°C) Hanks' balanced salt solution (HBSS), followed by 20 minutes in reduced-Ca^{2+} (20 μM) HBSS at room temperature.

The tissue was digested in reduced-Ca^{2+} (20 μM) HBSS solution containing collagenase (type I, 1750 U/ml), papain (9.5 U/ml), and bovine serum albumin (2 mg/ml) at 37°C for 20~30 minutes, followed by washing with Ca^{2+}-free HBSS to stop digestion. PASMCs were manually dispersed by trituration with a small-bore pipette in Ca^{2+}-free HBSS at room temperature. The cell suspension was placed on 25 mm glass coverslips in Ham's F-12 medium (with L-glutamine) supplemented with 0.5% fetal calf serum, 100 U/ml of streptomycin, and 0.1 mg/ml of penicillin. PASMCs from CH and normoxic animals were transiently (~24 hours) cultured inside a modular incubator chamber (Billups-Rothenberg, San Diego, CA) under 4% O_2/5% CO_2 and 21% O_2/5% CO_2, respectively.

Immunofluorescent Microscopy. Immunofluorescence analysis of TRPM8 and TRPC1 in the PASMCs was performed as previously described (Jiao et al., 2016). PASMCs grown on coverslips were washed and fixed in 4% paraformaldehyde for 30 minutes. The cells were then washed in phosphate-buffered saline (PBS) solution, permeabilized with 0.1% Triton- X in PBS for 10 minutes, and blocked with 2% bovine serum albumin for 1 hour. After fixation and blocking, the cells were incubated overnight at 4°C in with a primary rabbit polyclonal anti-TRPM8 (1:100; Alomone Labs, Jerusalem, Israel) and a primary mouse anti-TRPC1 (1:50; Santa Cruz Biotechnology, Dallas, TX), or without a primary antibody (PBS only, negative control). Thereafter, PASMCs were incubated with a fluorescence labeling conjugated anti-rabbit (Fluor 488; 1:1000; Beyotime Biotechnology, Jiangsu, People's Republic of China) and anti-mouse secondary antibodies (Fluor 555; 1:1000; Beyotime Biotechnology) for 1 hour, followed by 3 minutes of incubation with 4′, 6-diamidino-2-phenylindole to counterstain the nuclei.

Fluorescent images were captured using a Nikon Ti-E microscope (Nikon, Tokyo, Japan) equipped with epifluorescence attachments and an iXon DU-897 EMCCD camera (Andor, Belfast, United Kingdom). For the entire protocol, PASMCs of normoxia and CH rats were processed in parallel to reduce experimental variability, taking into account the potential differences in excitation intensity and exposure. The average fluorescent signals of various proteins were quantified for comparison.

Western Blot Analysis. Protein samples were separated with standard 12% SDS-polyacrylamide gels and transfer to a polyvinylidene fluoride membrane. The membrane was then probed overnight at 4°C with 5% nonfat dry milk and a rabbit monoclonal antibody specific for TRPC1 (1:1000; Abcam, Cambridge, MA), a polyclonal antibody against TRPM8 (1:300; Alomone Labs), or β-actin (1:5000; Cell Signaling Technology, Beverly, MA). After three washes with 0.1% Tris-buffered saline/Tween 20, the membrane was incubated with a secondary antibody (anti-rabbit from Abcam) for 1 hour at room temperature.

After three more washes, the bound antibodies were detected using enhanced chemiluminescence (Pierce, Rockford, IL), and the images for subsequent quantification were captured using the Gel Logic 200 image system (Kodak, New Haven, CT). The specificity of antibodies for TRPC1 and TRPM8 were verified as they detected a single major protein band at the predicted molecular weight.

Measurements of $[Ca^{2+}]_i$ of PASMCs. $[Ca^{2+}]_i$ of PASMCs were detected using the membrane-permeable Ca^{2+}-sensitive dye Fluo-3 AM. PASMCs were incubated with 5 μM Fluo-3/AM and 0.025% Pluronic F-127 for 45~60 minutes at room temperature in normal Tyrode solution containing 137 mM NaCl, 5.4 mM KCl, 2 mM $CaCl_2$, 1 mM $MgCl_2$, 10 mM HEPES, and 11.1 mM glucose. The cells were then washed thoroughly and rested for 15–30 minutes to allow for the complete deesterification of the cytosolic dye. Fluo-3 was excited at 488 nm, and emission light at >515 nm was detected using a Nikon TE2000U epifluorescence imaging system with a microfluometer (PTI, Tuckahoe, NY). $[Ca^{2+}]_i$ of PASMCs with 5–10 cells per field were monitored and recorded in each experimental trial. Fluo-3 fluorescence was calibrated for $[Ca^{2+}]_i$ as previously described elsewhere (Liu et al., 2012; Jiao et al., 2016).

Measurement of SOCE by Mn^{2+} Quenching of Fura-2. The rates of cation entry through TRPC1 and TRPM8 was quantified using the Mn^{2+} quenching technique as described elsewhere (Liu et al., 2013; Wang et al., 2015). PASMCs were incubated with 5 μM Fura-2 AM. Fura-2 was excited at the Ca^{2+}-insensitive isobestic point of 360 nm, and emission light was recorded at 510 nm using a Nikon TE2000U epifluorescence imaging system with a microfluometer (PTI). PASMCs were then bathed in a Ca^{2+}-free (with 0.1 mM EGTA) Tyrode solution containing 10 μM nifedipine. After a stable baseline fluorescent measurement was attained, 500 μM Mn^{2+} was applied through a concentration-clamp system with the multibarrel pipette positioned <50 μm from PASMCs. The rates of quenching of fura-2 fluorescence in PASMCs (5–10 cells per field) with/-without drug treatments were determined and compared.

Chemicals and Drugs. Icilin, phenylephrine, acetylcholine, and other chemicals were obtained from Sigma-Aldrich (St. Louis, MO) unless otherwise indicated. Ham's F-12 and fetal bovine serum were purchased from GIBCO (Auckland, New Zealand), and the fluorescent dye Fluo-3 AM and Fura-2 AM were obtained from Enzo Life Sciences International (Farmingdale, NY).

Statistical Analysis. Data are all represented as the mean ± S.E.M., and n indicates the number of animals, cell samples, or PA rings as specified in the text. $P < 0.05$ was considered statistically significant, and was determined via paired or unpaired Student's t tests or by one- or two-way analysis of variance as appropriate, using the software of Sigma Plot 11.0 (Systat Software, San Jose, CA).

Results

Verification of CHPH Rat Model

Rats exposed to 10% O_2 for 3 weeks developed PH and RV hypertrophy. RVSP was increased from 24.8 ± 0.8 mm Hg (n = 12) in the control animals to 61.3 ± 2.4 mm Hg (n = 12, $P < 0.01$) in the CH-exposed animals; the mean P_{Pa} was increased from 16.7 ± 0.8 (control, n = 12) to 34.7 ± 2.7 mm Hg (CH, n = 12, $P < 0.01$) (Fig. 1, C–D). RVMI, an index of RV hypertrophy, also increased significantly in the CH exposed rats (control: 25.7% ± 0.2%, n = 15; CH: 40.6% ± 1.1%, n = 13, $P < 0.01$) (Fig. 1E). These results confirmed that significant PH had developed in the CHPH rat model.

Alteration of TRPM8 and TRPC1 Expression in PASMCs of CHPH Rats

Our previous studies using real-time reverse-transcription polymerase chain reaction and Western blot showed that TRPM8 mRNA and protein are down-regulated while TRPC1 are up-regulated in the PAs of PH animal models (Lin et al., 2004; Liu et al., 2012; Yang et al., 2012; Liu et al., 2013). This is verified in the present study using Western blot analysis. TRPC1 protein expression was significantly higher (control: 0.03 ± 0.01, n = 3; CH: 0.27 ± 0.04, $P < 0.01$, n = 3) whereas TRPM8 protein expression was markedly reduced (control: 0.32 ± 0.03, n = 3; CH: 0.10 ± 0.02, n = 3) in the PAs of CHPH rats (Fig. 2, A and B).

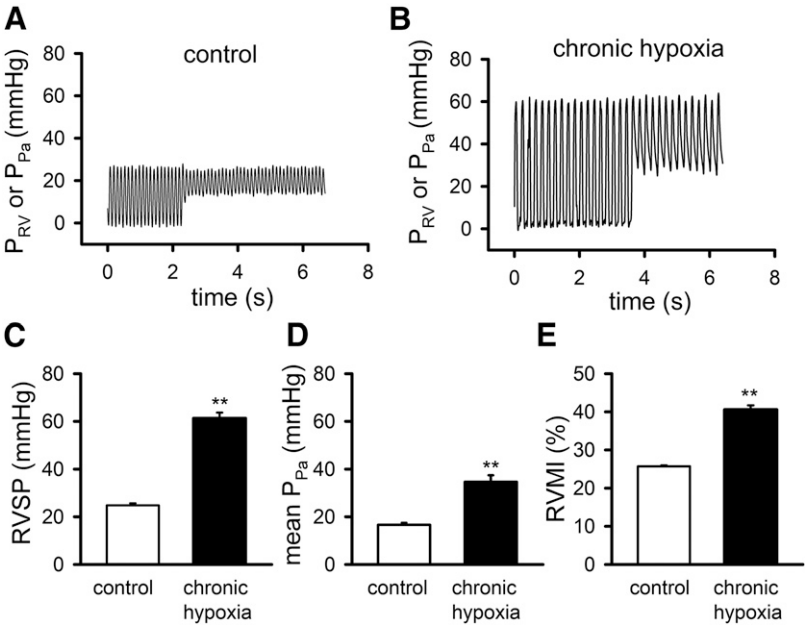

Fig. 1. Validation of pulmonary hypertension in rats exposed to CH for 3 weeks. (A and B) Representative tracings of right ventricular pressure (P_{RV}) and P_{Pa} recorded from a control and a CHPH rat. (C–E) The average values of RVSP, mean P_{Pa}, and RVMI of control (n = 11) and CH rats (n = 11). **Indicates a significant difference of $P <$ 0.01 compared with control.

Immunofluorescence analysis was performed to further characterize the expression of TRPM8 and TRPC1 proteins in PASMCs. Double-staining of PASMCs with specific antibodies against TRPC1 and TRPM8 showed clear expression of TRPM8 and TRPC1 in PASMCs (Fig. 2C). The fluorescent intensity of TRPM8 was significantly suppressed (control: 2699.50 ± 63.45, n = 72 cells; CH: 1237.21 ± 29.92, n = 80 cells, $P < 0.01$; Fig. 2D), whereas the signal of TRPC1 was

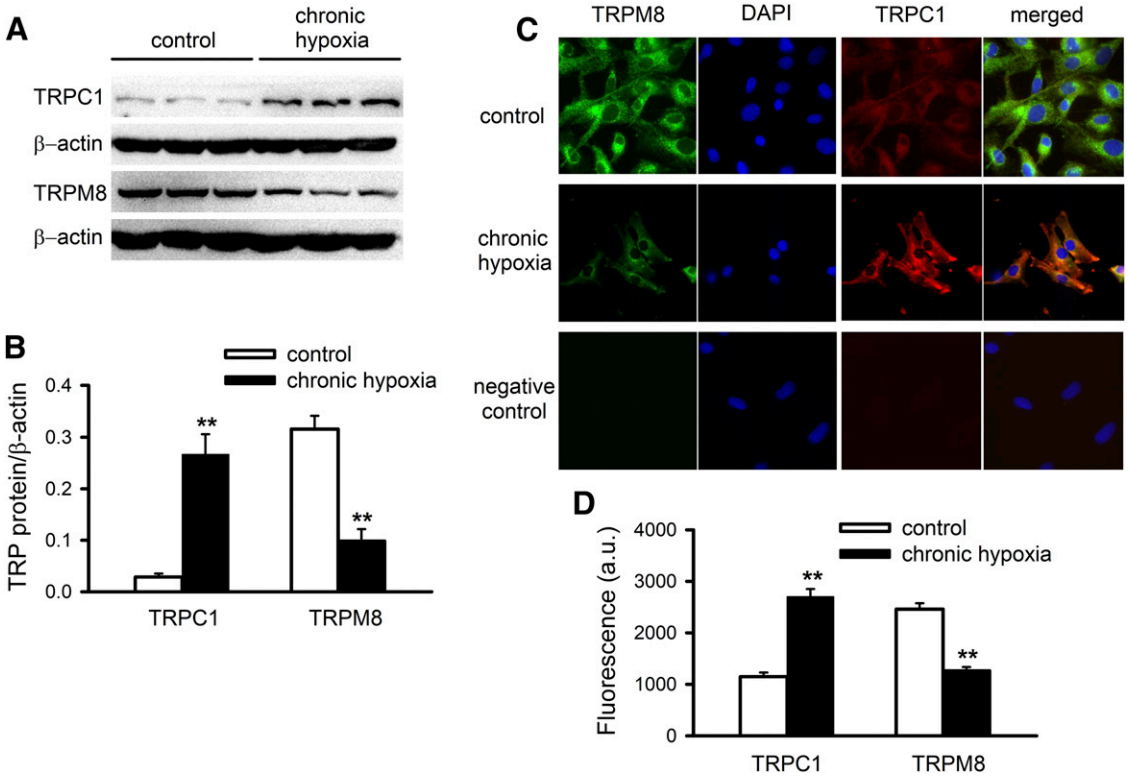

Fig. 2. Western blot and immunofluorescence analysis of TRPM8 and TRPC1 expression in PASMCs isolated from control and CHPH rats. (A) Western blot of TRPC1, TRPM8, and β-actin protein from PAs of normoxic and CHPH rats. (B) Bar graph showing the mean signals of TRPC1 and TRPM8 proteins from PAs of normoxic and CHPH rats (n = 3 rats in each group). (C) Representative immunofluorescent images of PASMCs from control and CHPH rats stained for TRPM8 (green), TRPC1 (red), and the nucleus (4′,6-diamidino-2-phenylindole [DAPI], blue). (D) Bar graph showing the average fluorescence intensity of TRPM8 and TRPC1 measured in control (n = 72) and CH PASMCs (n = 80). Primary cultures of PASMCs were obtained from three control and three CHPH rats. **Indicates a significant difference of $P < 0.01$ compared with control.

increased robustly in PASMCs of CHPH rats (control: 1257.57 ± 37.03, n = 72 cells; CH: 2511.79 ± 60.6, n = 80 cells, $P < 0.01$; Fig. 2D). These results show that TRPM8 and TRPC1 are coexpressed in PASMCs; TRPC1 expression is up-regulated and TRPM8 expression is markedly decreased during CHPH.

Alteration in TRPM8-Mediated Cation Entry and SOCE in PASMCs of CHPH Rats

TRPM8-mediated cation entry in PASMCs was assessed by Mn^{2+} quenching of Fura-2 fluorescence. Activation of TRPM8 with the specific TRPM8 agonist icilin (10 μM, 15-minute preincubation) caused a significant increase in the rate of Mn^{2+} quenching. The percentage reduction of the fluorescence signal measured 500 seconds after Mn^{2+} application was −32.27% ± 2.2%, and the maximal rate of Mn^{2+} quenching was −0.064% ± 0.007% per second in control PASMCs (n = 13). They were significantly reduced to −21.38% ± 1.90% and −0.045% ± 0.005% per second (n = 13, $P < 0.01$), respectively, in CHPH-PASMCs (Fig. 3, A, C, and D).

In contrast, Mn^{2+} quenching induced by activation of SOCE with cyclopiazonic acid (10 μM CPA, 15-minute preincubation) was significantly enhanced in PASMCs of CHPH rats (control: −34.10% ± 1.70%, n = 11; CH: −69.78% ± 0.81%, n = 12, $P < 0.01$, Fig. 3, B–D). The maximal rate of Mn^{2+} -induced quenching was increased from −0.062% ± 0.004% per seconds (n = 13,) in control to −0.102% ± 0.004% per second (n = 12, $P < 0.01$, Fig. 3) in hypoxic PASMCs. These findings clearly show that the functional activity of TRPM8 and TRPC1 in PASMCs are altered in CHPH.

TRPM8 Activation Attenuates SOCE-Mediated PA Vasoconstriction

The functional interaction between TRPM8 activation and SOCE was first examined in endothelium-denuded PAs of normoxic rats preincubated with 10 μM CPA for 15 minutes in Ca^{2+}-free and 3 μM nifedipine-containing solution. Two millimolars Ca^{2+} was then reintroduced to elicit SOCE-mediated vasoconstriction. Application of icilin (0.1–100 μM) caused concentration-dependent relaxation of CPA-precontracted PAs (Fig. 4, A and C). The maximal percentage relaxation (E_{max}) was −98.52% ± 11.69%, and the EC_{50} of vasodilation was 6.09 ± 0.66 μM (n = 15). The vasorelaxant effect of icilin was completely abolished by the TRPM8 antagonist N-(3-aminopropyl)-2-([(3-methylphenyl)methyl])-oxy-N-(2-thienylmethyl) benzamide hydrochloride salt (AMTB, 10 μM) (Lashinger et al., 2008) (Fig. 4B).

To further investigate the mechanism of TRPM8 activation on inhibiting SOCE, we examined the effects of icilin and the SOCE blocker gadolinium (Gd^{3+}) on CPA-induced contraction in control and CHPH rats. In control PAs, application of 10 μM icilin caused significant relaxation of the CPA-induced contraction from 54.60% ± 1.00% of the maximal KCl response to 40.14% ± 1.33% (n = 13, $P < 0.01$) (Fig. 5, A and E). Addition of 0.4 μM Gd^{3+} caused further relaxation to 31.72% ± 1.09% (n = 13, $P < 0.01$). In contrast, application of Gd^{3+} alone inhibited CPA-induced contraction (33.87% ± 1.20%, n = 13, $P < 0.01$) to a level similar to that caused by icilin plus Gd^{3+}. Subsequent addition of icilin failed to cause further relaxation (31.46% ± 1.13%) (Fig. 5, B and F), suggesting the effect of icilin is dependent on the availability of SOCE.

In the PAs of CHPH rats, CPA-induced maximal response was significantly augmented (control: 54.61% ± 1.03% of maximal KCl response, n = 13; CH: 98.76% ± 2.43%, n = 13, $P < 0.01$) (Fig. 5, C and D). Icilin or Gd^{3+} caused greater relaxation compared with the control PAs (Fig. 5, G and H). Similar to the control PAs, application of icilin after Gd^{3+} was ineffective to cause further relaxation of the CH PAs (Fig. 5H). These results provide the evidence that TRPM8 activation with icilin inhibits SOCE in PAs, and inhibition is enhanced during PH.

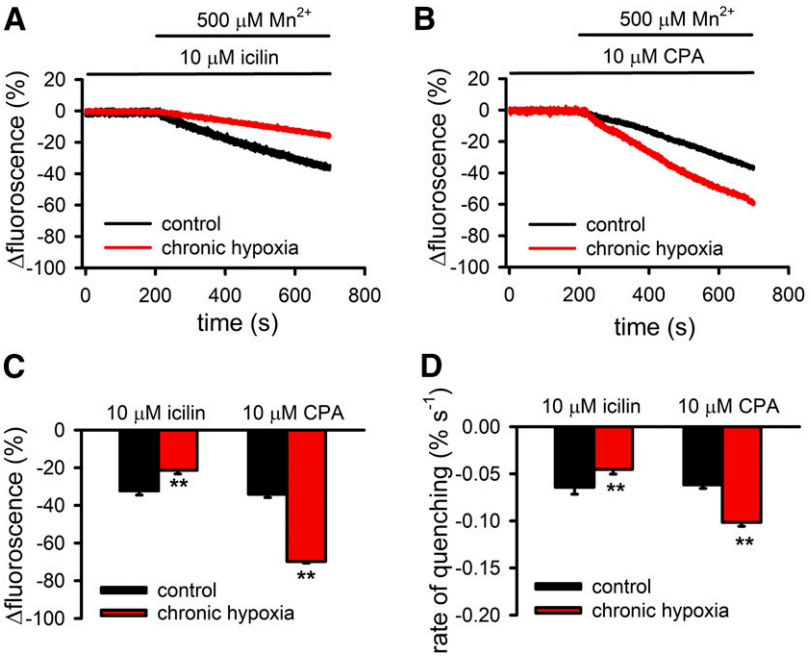

Fig. 3. Characterization of icilin and CPA-induced cation entry by measuring Mn^{2+} quenching of Fura-2 fluorescence in PASMCs of control and CHPH rats. (A and B) Representative tracings of icilin and CPA-induced cation entry recorded in control and CH PASMCs. (C) Average percentage of reduction of fluorescence measured 500 seconds after application of Mn^{2+} in control and CH PASMCs pretreated with 10 μM icilin (control: n = 13 and CH: n = 15 experiments) or 10 μM CPA (control: n = 11 and CH: n = 12 experiments). (D) The average maximum rate of quenching measured in the various groups of treated cells in *C*. **Indicates a significant difference of $P < 0.01$ compared with control. Each group comprised at least 10 dishes of PASMCs from six rats.

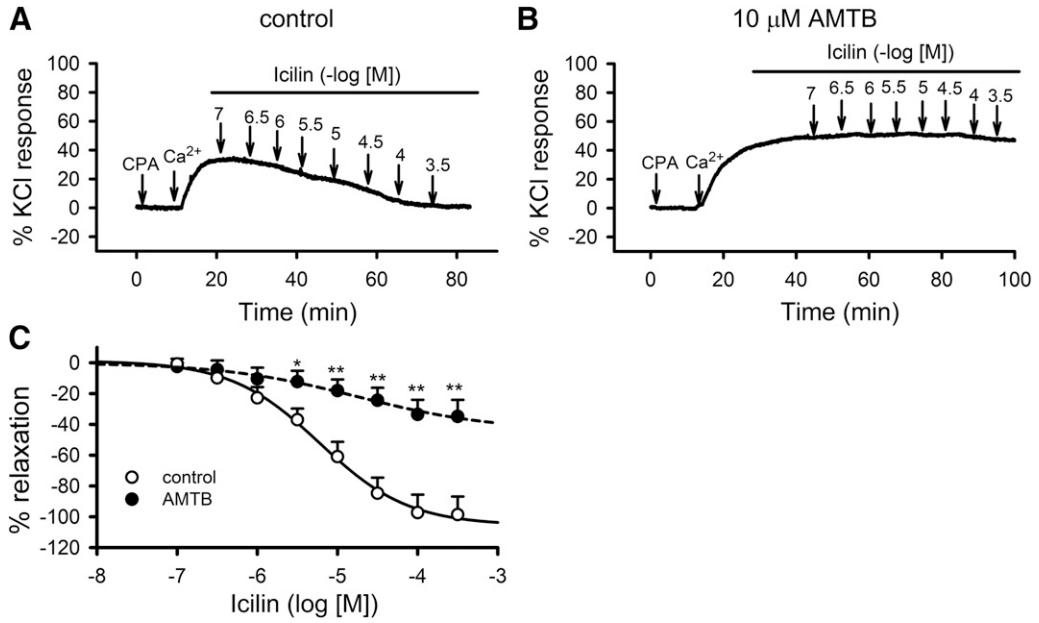

Fig. 4. The effect of icilin-induced activation of TRPM8 on the SOCE-mediated vasoconstriction in rat pulmonary arterial rings. (A and B) Typical traces of icilin-induced concentration-dependent relaxation of CPA precontracted endothelium-denuded PAs in the absence or presence of the TRPM8 channel antagonist AMTB (10 μM). (C) Average percentage of relaxation elicited by icilin in PAs precontracted with CPA (control: n = 15; AMTB: n = 11). Icilin-induced relaxation is expressed as the percentage of decrease in the maximum tension elicited by reapplication of 2 mM Ca^{2+} to the CPA-pretreated PAs. **Indicates a significant difference of $P < 0.01$ compared with control. The downward arrow indicates the addition of the reagent and the concentration attained thereafter. Each group consisted of cells from six to eight rats.

TRPM8 Activation Attenuates Endothelin-1-Induced PAs Contraction in Control and CH-Exposed Rats

Previous studies showed that endothelin-1 (ET-1) activates Ca^{2+} release and SOCE in PASMCs (Liu et al., 2012). To evaluate the interactions between TRPM8 and SOCE elicited by a natural agonist, we examined the effect of icilin on ET-1-induced contraction (Fig. 6, A–D).

Consistent with our previous observations (Liu et al., 2012; Wang et al., 2015; Jiao et al., 2016), ET-1 induced contraction was increased in PAs of CHPH rats. Icilin caused dramatic relaxation of ET-1 precontracted PAs in the presence of nifedipine, and subsequent application of Gd^{3+} caused additional relaxation (icilin: $-31.50\% \pm 1.12\%$, $n = 15$; icilin + Gd^{3+}: $-49.56\% \pm 1.41\%$, $n = 15$, Fig. 6G). The percentage inhibition induced by icilin and icilin plus Gd^{3+} were significantly enhanced in CH PAs (icilin: $-42.84\% \pm 1.75\%$, $n = 18$; icilin + Gd^{3+}: $-68.16\% \pm 2.38\%$, $n = 18$, $P < 0.01$). Moreover, application of Gd^{3+} alone caused relaxation of PAs of control rats and CHPH rats to a level similar to that elicited by icilin plus Gd^{3+} (Fig. 6, B and D). Application of icilin in the presence of Gd^{3+} failed to cause further relaxation (Fig. 6, F and H).

These results provide evidence suggesting that icilin inhibits SOCE activated by ET-1. It has to mention, however, TRPM8 activation with icilin may affect other ET-1-dependent signaling pathways, and Gd^{3+} may affect some unknown conductance, which may contribute to PA relaxation under certain conditions.

Effects of TRPM8 Activation on CPA-Induced Cation Entry and Ca^{2+} Transients of PASMCs. To further investigate the inhibitory effects of TRPM8 activation on SOCE, CPA-induced cation entry was monitored using the Mn^{2+} quenching technique in PASMCs. Icilin preincubation attenuated the CPA-induced Mn^{2+} quenching in PASMCs of control and CHPH rats (Fig. 7, A and B). The maximal rate of Mn^{2+} quenching was reduced from $-0.062\% \pm 0.004\%$ per second ($n = 8$) to $-0.039\% \pm 0.003\%$ per second ($n = 8$) in the control PASMCs; and from $-0.102\% \pm 0.004\%$ per second ($n = 9$) to $-0.06\% \pm 0.003\%$ per second ($n = 9$) in the CH PASMCs (Fig. 7D). The inhibitory effect of icilin was greater in PASMCs of CHPH rats ($-38.98\% \pm 1.93\%$, $n = 8$, $P < 0.01$) compared with the control rats ($-28.99\% \pm 4.07\%$, $n = 9$, $P < 0.01$) (Fig. 7C).

TRPM8-induced inhibition of SOCE was further evaluated by measuring the CPA-induced Ca^{2+} transients in PASMCs. Application of CPA (10 μM) to PASMCs in Ca^{2+}-free and nifedipine-containing solution activated a large Ca^{2+} release transient. Subsequent reintroduction of 2 mM Ca^{2+} elicited a sustained Ca^{2+} response due to Ca^{2+} influx (Fig. 8A). Preincubation with icilin (10 μM, 15 minutes) caused a reduction in the baseline $[Ca^{2+}]_i$ but had no effect on CPA-induced Ca^{2+} release (Fig. 8E). However, the CPA-induced Ca^{2+} influx was significantly reduced (control: 165.1 ± 8.1 nM, $n = 8$; icilin: 114.8 ± 4.8 nM, $n = 8$) (Fig. 8F). The resting $[Ca^{2+}]_i$ was significantly higher in CH PASMCs, suggesting enhanced SOCE (control: 194.3 ± 12.9 nM, $n = 8$; CH: 318.4 ± 20.4 nM, $n = 10$, $P < 0.01$). CPA-induced Ca^{2+} release and Ca^{2+} influx were significant greater in CH PASMCs (Fig. 8B).

Similar to the control PASMCs, icilin had no effect on CPA-induced Ca^{2+} release but caused significant reduction in the Ca^{2+} influx in PASMCs (Fig. 8, E and F). The inhibitory effect of icilin on CPA-induced SOCE was more pronounced in CH PASMCs (percentage inhibition: control: $-28.78\% \pm 4.91\%$, $n = 8$; CH: $-45.32\% \pm 2.36\%$, $n = 10$, $P < 0.05$) (Fig. 8G). Moreover, the effect of icilin on CPA-induced Ca^{2+} influx was completely blocked by AMTB in the control and CH cells (Fig. 8, C and D).

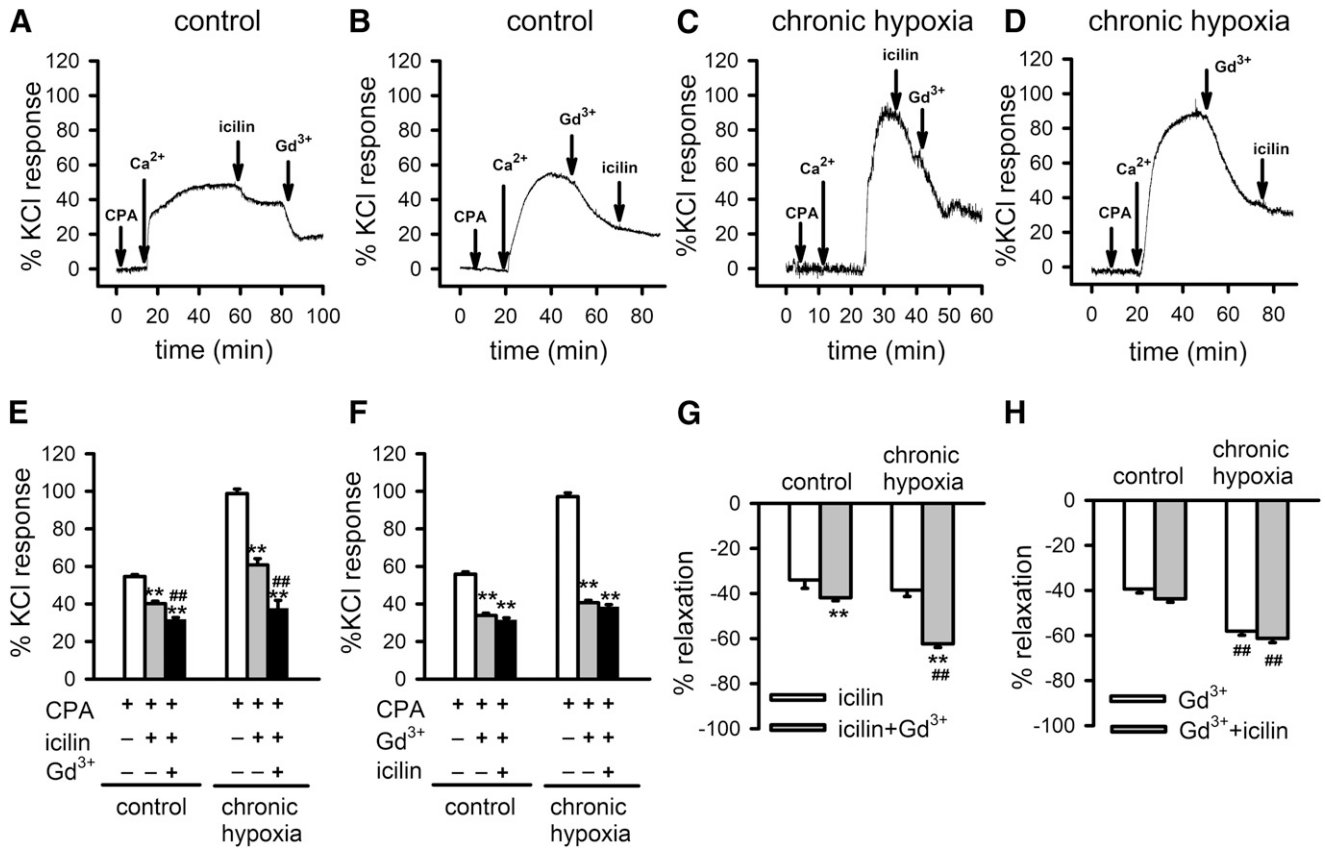

Fig. 5. The relaxant effects of icilin and Gd^{3+} in CPA precontracted PAs of control and CHPH rats. (A and B) Typical tracings of icilin-induced vasorelaxation in CPA (10 μM) precontracted PAs of control rats before or after the application of 0.4 μM Gd^{3+}. (C and D) Representative tracings of icilin-induced vasorelaxation in CPA precontracted PAs of CHPH rats before or after the application of Gd^{3+}. (E) Average values of CPA-induced contraction measured before and after the application of icilin and the subsequent addition of Gd^{3+} in PAs of control and CHPH rats (control: $n = 13$, and CH: $n = 13$). (F) Average values of CPA-induced contraction measured before and after the application of Gd^{3+} and the subsequent addition of icilin in PAs of control and CHPH rats (control: $n = 13$, and CH: $n = 14$). **Indicates a significant difference of $P < 0.01$ between CPA-induced contraction before and after drug treatment. ##Indicates a significant difference ($P < 0.01$) between the icilin and icilin + Gd^{3+} treatments. (G) Percentage relaxation of CPA-induced contractions caused first by icilin and then by icilin + Gd^{3+} and (H) caused first by $Gd^{3+}$and then by Gd^{3+} + icilin in PAs of control and CH-exposed rats. **Indicates a significant difference ($P < 0.01$) between icilin and icilin + Gd^{3+}. ##Indicates a significant difference ($P < 0.01$) between the response in the control and CH PAs. The downward arrow indicates the addition of the reagent and its continued presence throughout the remainder of the experiment. Each group consisted of PAs from six to eight rats.

These results provide the direct evidence that TRPM8 activation can effectively inhibit SOCE, and this effect is potentiated when SOCE is up-regulated during CHPH.

Discussion

The present study tested the hypothesis that activation of TRPM8 can modulate pulmonary vasoreactivity through the regulation of SOCE in PASMCs and evaluated the change of this TRPM8-dependent mechanism in CHPH. The major findings are: 1) TRPM8 expression was down-regulated and the TRPM8-mediated cation entry was reduced in the PASMCs of CHPH rats; 2) activation of TRPM8 with icilin caused concentration-dependent relaxation of CPA and ET-1-precontracted PAs, and the vasorelaxant effect of icilin was blocked by the SOCE antagonist Gd^{3+}; 3) icilin suppressed CPA-induced cation entry and Ca^{2+} transients in PASMCs, and this inhibitory effect of icilin was abolished by the TRPM8-specific antagonist AMTB; and 4) the TRPM8-mediated inhibitory effects on SOCE were significantly augmented in PAs and PASMCs of CHPH rats, in which SOCE was significantly augmented. These results show for the first time that activation of TRPM8 can cause relaxation of PA through SOCE inhibition. Because SOCE plays many important roles crucial to the enhanced vasoconstriction and vascular remodeling in PH (Lin et al., 2004; Yu et al., 2004; Liu et al., 2012; Xia et al., 2014), the down-regulation of TRPM8 in PASMCs during CHPH may minimize the TRPM8-dependent inhibition and allow unimpeded SOCE activity for PH development.

We have previously shown that TRPM8 is highly expressed in PA and aorta and that activation of TRPM8 with menthol elicits Ca^{2+} influx in PASMCs (Yang et al., 2006). Subsequent studies by others in systemic arteries showed that TRPM8 agonists menthol and icilin can elicit small vasoconstriction in resting arteries and vasorelaxation in arteries precontracted with contractile agonists (Johnson et al., 2009; Silva et al., 2015; Melanaphy et al., 2016). Vasoconstriction induced by the TRPM8 agonists in resting arteries is due to Ca^{2+} mobilization (Yang et al., 2006; Melanaphy et al., 2016), but the TRPM8-mediated vasorelaxation is not well understood. Several mechanisms, including activation of Ca^{2+}-independent phospholipase A^2 or inhibition of voltage-gated Ca^{2+} channels (VDCC) and the RhoA/Rho kinase pathway

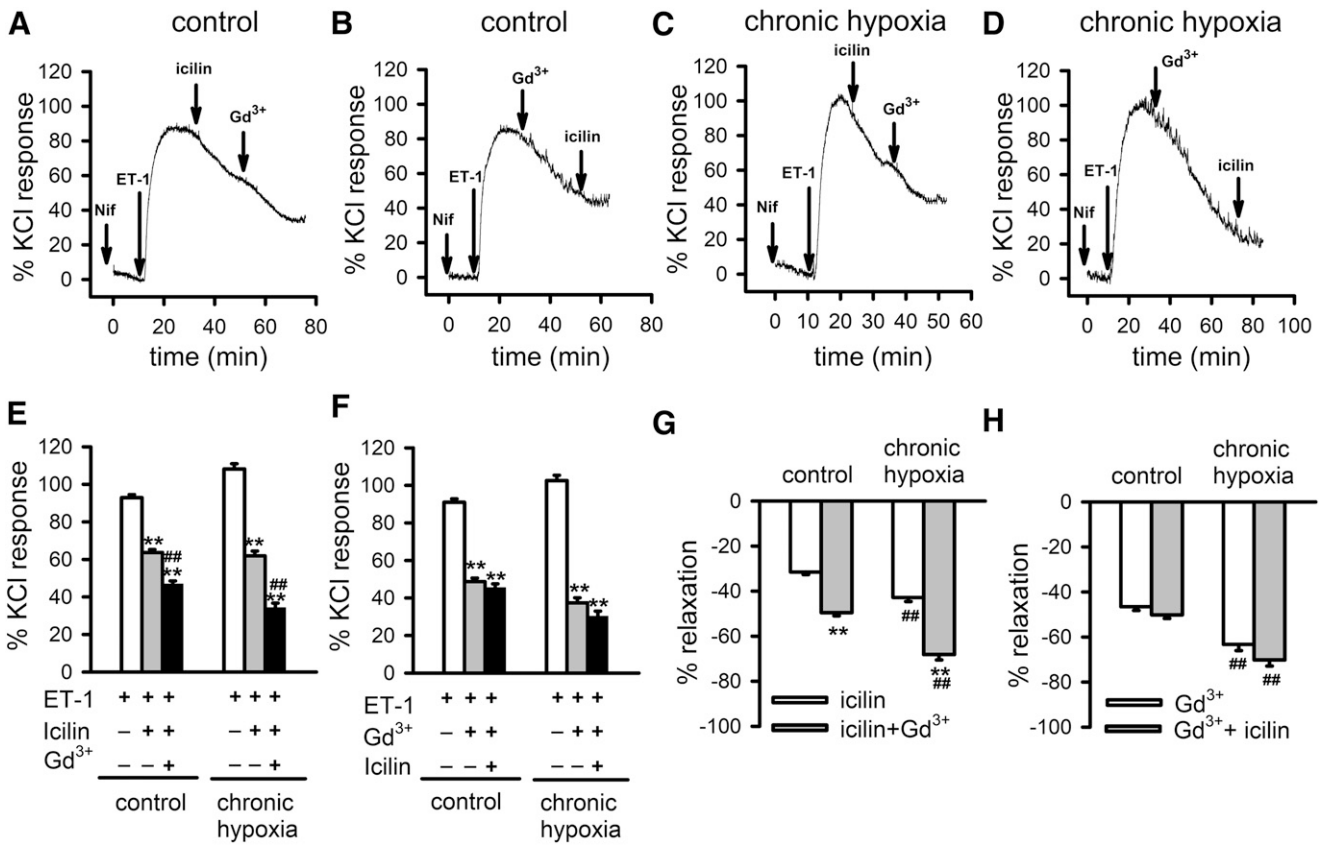

Fig. 6. The relaxant effects of icilin and Gd^{3+} in ET-1 precontracted PAs of control and CHPH rats. (A and B) Typical tracings of icilin-induced vasorelaxation in ET-1 (10 nM) precontracted PAs of control rats before or after the application of 0.4 μM Gd^{3+}. (C and D) Representative tracings of icilin-induced vasorelaxation in ET-1 precontracted PAs of CHPH rats before or after the application of Gd^{3+}. (E) Average values of ET-1-induced contraction measured before and after the application of icilin and after the subsequent addition of Gd^{3+} in PAs of control and CHPH rats (control: $n = 15$, and CH: $n = 18$). (F) Average values of ET-1-induced contraction measured before and after the application of Gd^{3+} and after the subsequent addition of icilin in PAs of control and CHPH rats (control: $n = 16$, and CH: $n = 12$). **Indicates a significant difference ($P < 0.01$) between ET-1–induced contraction before and after drug treatment. ##Indicates a significant difference ($P < 0.01$) between the icilin and icilin + Gd^{3+} treatments. (G) Percentage relaxation caused first by icilin and then by icilin + Gd^{3+}, or (H) caused first by $Gd^{3+}$and then by Gd^{3+} + icilin in PAs of control and CH-exposed rats. **Indicates a significant difference ($P < 0.01$) between icilin and icilin + Gd^{3+}. ##Indicates a significant difference ($P < 0.01$) between the response in the control and CH PAs. The downward arrow indicates the addition of the reagent and its continued presence throughout the remainder of the experiment. Each group consisted of 6–10 rats.

(Johnson et al., 2009; Cheang et al., 2013; Sun et al., 2014; Silva et al., 2015; Melanaphy et al., 2016), have been proposed for the menthol-induced vasorelaxation. A recent study in rat tail arteries showed that the TRPM8 agonist menthol has the dual effect of vasoconstriction mediated by TRPM8 activation and vasorelaxation related to L-type Ca^{2+} channel inhibition; vasoconstriction is the primary response of TRPM8 activation caused by Ca^{2+} release from the SR (Melanaphy et al., 2016).

The icilin-induced vasorelaxation reported here is unlikely related to VDCC inhibition. Icilin is a more specific TRPM8 agonist, and it does not inhibit VDCC at the concentration used (10 μM) (Baylie et al., 2010), even though it partially inhibits VDCC in rat tail VSMCs at a higher concentration (50 μM) (Melanaphy et al., 2016). The involvement of VDCC was further precluded by including nifedipine in all our experiments. Moreover, submicromolar Gd^{3+}, which is ineffective for VDCC inhibition but highly potent for SOCE inhibition (Flemming et al., 2003; Lin et al., 2016), completely blocked the icilin-induced response. Our observation of TRPM8-specific vasorelaxation of PAs is consistent with a previous study in mouse mesenteric arteries that showed icilin caused significant inhibition of contraction induced by U46619 (9,11-dideoxy-9α,11α-methanoepoxy prostaglandin F2α), and the effect was absent in the arteries of *trpm8*$^{-/-}$ mice (Sun et al., 2014).

The present study suggests that the TRPM8-induced PA relaxation is mediated via SOCE inhibition. This is supported by several lines of converging evidence. At the tissue level, icilin caused relaxation of PA precontracted by the SR Ca^{2+} -ATPase inhibitor CPA or by ET-1, which activates SOCE through the phospholipase C-IP_3 and Ca^{2+} release signaling cascade (Zhang et al., 2003, 2004b; Liu et al., 2012; Jiao et al., 2016). The vasorelaxant responses were completely abolished when SOCE was inhibited by submicromolar Gd^{3+} (Flemming et al., 2003; Liu et al., 2012; Lin et al., 2016). At the cellular level, icilin suppressed CPA-induced Mn^{2+} quenching and Ca^{2+} influx transients, and the effect could be abolished by the TRPM8 antagonist AMTB (Lashinger et al., 2008; Melanaphy et al., 2016).

Our observation in PASMCs is different from those in LNCaP cells, where stimulation of TRPM8 with menthol or icilin caused Ca^{2+} release from ER and SOCE activation (Thebault et al., 2005). In our study, SOCE was maximally activated by CPA before TRPM8 activation; hence, icilin did

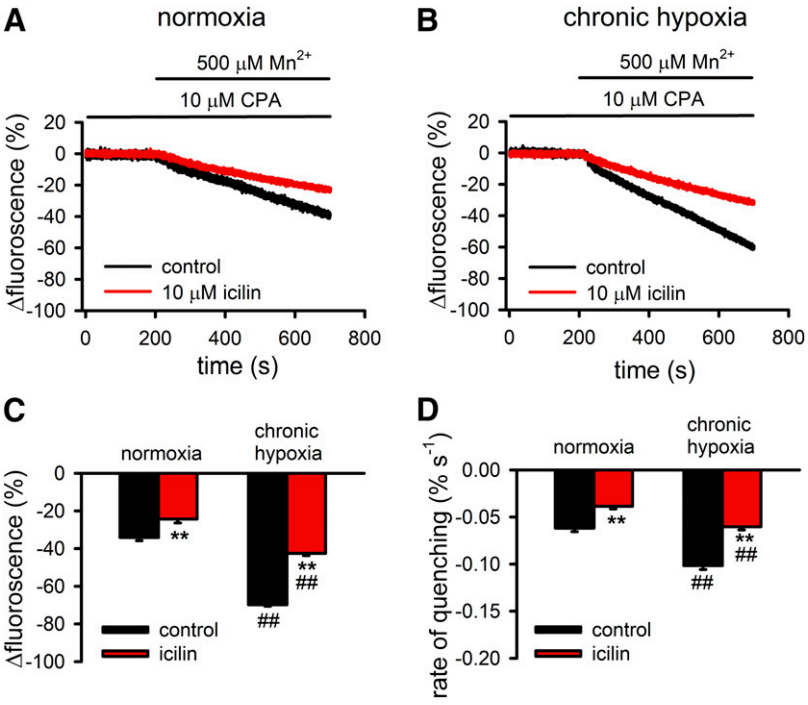

Fig. 7. Effect of icilin on CPA-induced SOCE measured by Mn^{2+} quenching of Fura-2 fluorescence in PASMCs of control and CHPH rats. (A and B) Representative tracings of CPA-induced Mn^{2+} quenching in PASMCs of control and CHPH rats with or without preincubation with icilin. (C) Average percentage reduction of fluorescence measured at 500 seconds after Mn^{2+} application in control and CH PASMCs with or without icilin (10 μM) (control: n = 8, and CH: n = 9 experiments). (D) Maximum rate of quenching measured in PASMCs of control and CHPH rats. **Indicates a significant difference ($P < 0.01$) between PASMCs with and without icilin treatment. ##Indicates a significant difference ($P < 0.01$) between the PASMCs of normoxic and CH rats. Each group comprised at least eight dishes of PASMCs from six rats.

not cause further activation of SOCE. Under these conditions, icilin caused a TRPM8-dependent inhibition of SOCE in PASMCs. It is important to note, however, that this mechanism does not only operate under the condition of SR Ca^{2+}-ATPase inhibition because similar TRPM8-mediated vasorelaxation was observed in PA contracted with ET-1.

Despite these observations, how TRPM8 modulates SOCE is unclear. There are several possible mechanisms. First, it could be related to the functional interactions of TRPM8 and the SOCE complex. SOCE is mediated by intermolecular interactions between many plasma membrane and SR proteins, including the SR Ca^{2+} sensors STIM1 and STIM2 (Song et al., 2011; Ogawa et al., 2012), the Ca^{2+} permeating channels Orai1, Orai2, and TRPC (Ng et al., 2010; Ng et al., 2012; Fernandez et al., 2015), and a range of other associated proteins (Soboloff et al., 2012). Activation of TRPM8 in the SR and/or plasma membrane may interfere the formation or function of the SOCE complex. However, direct molecular interactions of TRPM8 with STIM, Orai, or TRPC channels and their associated proteins have not been established.

TRPM8 may also affect SOCE indirectly through channel-dependent and independent mechanisms. It had been shown that activation of SR-resident TRPM8 couples Ca^{2+} release to mitochondrial Ca^{2+} uptake to regulate ROS generation and oxidative stress in non-smooth muscle cells and VSMCs (Bidaux et al., 2015, 2016; Xiong et al., 2017). In non-smooth muscle cells, oxidative states can regulate STIM-Orai coupling through redox-dependent modification of cysteine residues in STIM and Orai proteins (Cioffi, 2011; Nunes and Demaurex, 2014; Alansary et al., 2016). In particular, *S*-glutathionylation of cysteine residue C56 close to the EF-hand of STIM1 can reduce the Ca^{2+} binding affinity of STIM1, leading to STIM1 oligomerization and activation (Hawkins et al., 2010); and oxidation of the cysteine residue C195 of Orai1 can lock the channel in a closed conformation to block Ca^{2+} influx (Bogeski et al., 2010; Alansary et al., 2016). Redox-regulation of TRPC channels, including TRPC1, TRPC3, TRPC4, and TRPC5, has also been observed in several cell types (Yoshida et al., 2006; Cioffi, 2011; Kozai et al., 2014; Badr et al., 2016). Moreover, TRPM8 activation can antagonize angiotensin II–induced mitochondrial respiratory dysfunction and excess ROS generation in mouse VSMCs (Xiong et al., 2017). Hence, it is possible that TRPM8 activation may trigger a similar ROS-dependent mechanism to modulate SOCE in PASMCs and PA contraction.

In addition, TRPM8 is known to activate other channel-independent signaling mechanisms. For example, stimulation of TRPM8 can cause trapping of the small GTPase Rap1 (Genova et al., 2017), which is required for the maintenance of vascular tone (Lakshmikanthan et al., 2014); TRPM8 activation can also affect RhoA/Rho kinase pathway in systemic vasculature (Sun et al., 2014). Hence, future studies are warranted for studying TRPM8-dependent regulation of ROS and other signaling pathways in the modulation of SOCE and relaxation in pulmonary vasculatures.

TRPM8 activation with icilin caused greater inhibition of SOCE in the PAs and PASMCs of CHPH rats, despite the down-regulation of TRPM8 expression. One possible explanation is that TRPM8 expression in normoxic PA is high and may be in excess, so the reduced number of TRPM8 in CH PAs is still sufficient to effectively inhibit SOCE when activated by a potent agonist like icilin. This is consistent with our previous finding that TRPM8 is the most abundant channel among the eight TRPM subtypes in PAs (Yang et al., 2006). Moreover, SOCE activity is dramatically enhanced in CH PAs (Lin et al., 2004; Wang et al., 2015). Hence, TRPM8 activation can cause a stronger inhibition of SOCE in CHPH-PAs compared with the control.

Increased SOCE activity has been demonstrated consistently in PASMCs of PH models and IPAH patients (Lin et al., 2004; Yu et al., 2004; Zhang et al., 2007; Liu et al., 2012; Jiao et al., 2016). It is accompanied with the up-regulation of the

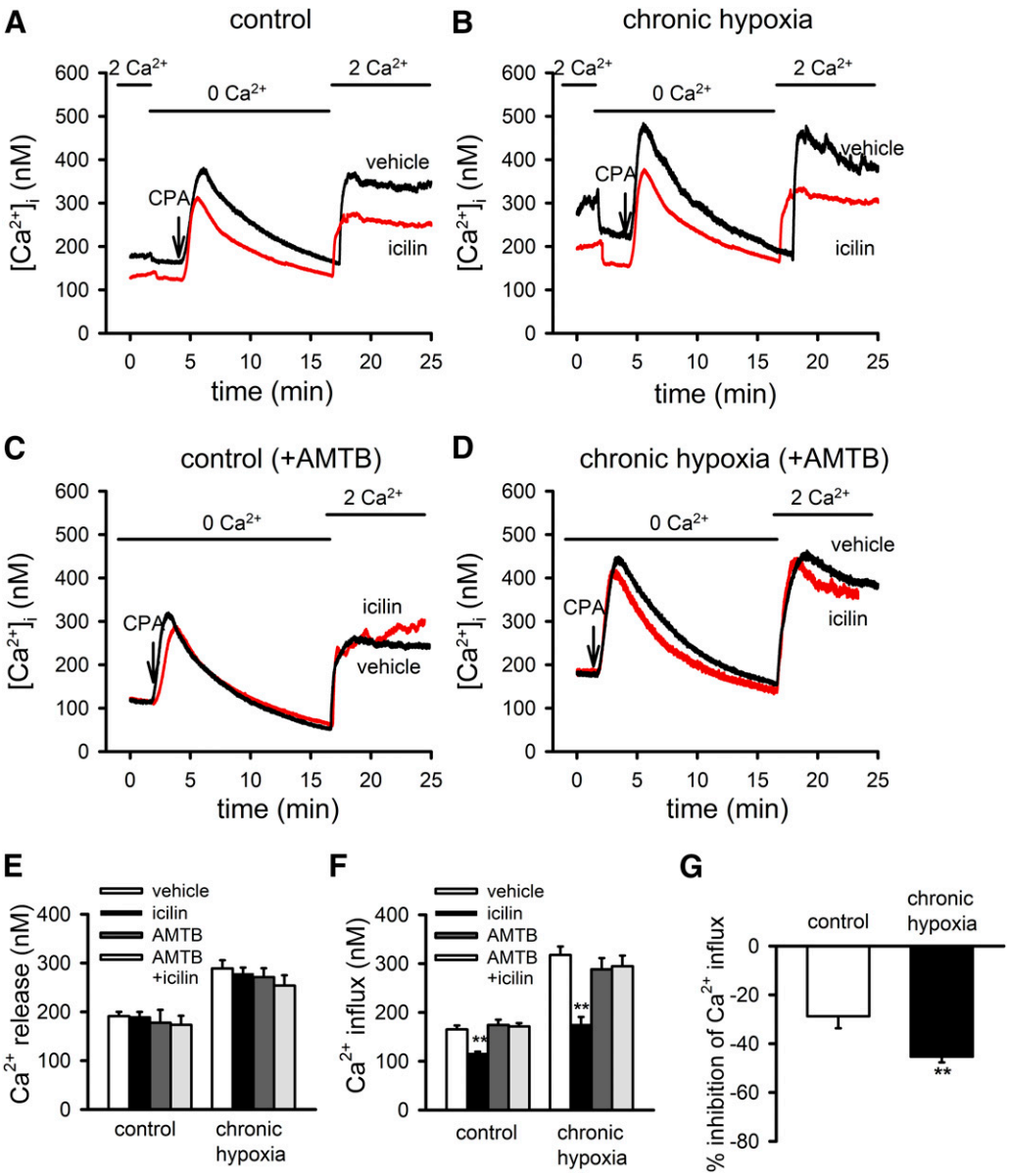

Fig. 8. The effect of icilin on CPA-induced Ca^{2+} transients in PASMCs of control and CHPH rats. (A and B) Representative tracings of CPA-induced Ca^{2+} transients in PASMCs of control and CHPH rats with or without pretreatment with icilin. (C and D) Representative tracings of CPA-induced Ca^{2+} transients in PASMCs with or without icilin in the presence of the TRPM8 channel antagonist AMTB. (E and F) Average values of the peak Ca^{2+} transients elicited by CPA-induced Ca^{2+} release and Ca^{2+} entry in PASMCs of control and CHPH rats in the presence or absence of icilin or AMTB. **Indicates a significant difference ($P < 0.01$) between PASMCs with and without icilin pretreatment. (G) Percentage inhibition of CPA-induced Ca^{2+} entry caused by icilin. **Indicates a significant difference ($P < 0.01$) between PASMCs of control and CHPH rats. The downward arrow indicates the addition of the reagent and its continued presence throughout the remainder of the experiment. Each group comprised 8–10 dishes of PASMCs from eight rats.

SOCE channels TRPC1, TRPC6, Orai1, and Orai2 in CHPH rats (Lin et al., 2004; Wang et al., 2017); TRPC1 and TRPC4 in monocrotaline-induced PH rats (Liu et al., 2012); TRPC4 and STIM1 in the high-altitude CH neonatal lamb (Parrau et al., 2013); and STIM2, Orai2, and TRPC6 in IPAH-PASMCs (Song et al., 2011; Fernandez et al., 2015) The augmentation of SOCE plays many critical roles in the elevated vascular tone, enhanced vasoreactivity, and vascular remodeling in PH (Lin et al., 2004; Fernandez et al., 2012; Kuhr et al., 2012; Liu et al., 2012; Xia et al., 2014).

Down-regulation of TRPM8 has been observed in CHPH and monocrotaline-induced PH (Yang et al., 2012; Liu et al., 2013). The decrease in TRPM8 expression occurs in the early stage of PH, preceding the increase in RVSP and RV mass index, and it remains at a low level throughout PH development (Liu et al., 2013). Because TRPM8 activation inhibits SOCE, down-regulation of TRPM8 during PH could reduce the inhibitory influence on SOCE. With the concomitant up-regulation of SOCE during PH, TRPM8 down-regulation may allow unimpeded SOCE activity for increasing pulmonary vascular tone, vasoreactivity, and vascular remodeling.

In conclusion, we have revealed a novel mechanism of TRPM8-dependent inhibition of SOCE in rat pulmonary vasculatures, and down-regulation of TRPM8 may play a

significant role in facilitating CHPH development. The possible role of TRPM8 down-regulation in other forms of PH requires future investigations.

Authorship Contributions

Participated in research design: Mu, M.-J. Lin, Sham.

Conducted experiments: Mu, D.-C. Lin, Zheng, Jiao.

Performed data analysis: Mu, D.-C. Lin.

Wrote or contributed to the writing of the manuscript: Sham, Mu, M.-J. Lin.

References

Alansary D, Schmidt B, Dörr K, Bogeski I, Rieger H, Kless A, and Niemeyer BA (2016) Thiol dependent intramolecular locking of Orai1 channels. *Sci Rep* **6**:33347.

Badr H, Kozai D, Sakaguchi R, Numata T, and Mori Y (2016) Different contribution of redox-sensitive transient receptor potential channels to acetaminophen-induced death of human hepatoma cell line. *Front Pharmacol* **7**:19.

Baylie RL, Cheng H, Langton PD, and James AF (2010) Inhibition of the cardiac L-type calcium channel current by the TRPM8 agonist, (−)-menthol. *J Physiol Pharmacol* **61**:543–550.

Bidaux G, Borowiec AS, Gordienko D, Beck B, Shapovalov GG, Lemonnier L, Flourakis M, Vandenberghe M, Slomianny C, Dewailly E, et al. (2015) Epidermal TRPM8 channel isoform controls the balance between keratinocyte proliferation and differentiation in a cold-dependent manner. *Proc Natl Acad Sci USA* **112**: E3345–E3354.

Bidaux G, Borowiec AS, Prevarskaya N, and Gordienko D (2016) Fine-tuning of eTRPM8 expression and activity conditions keratinocyte fate. *Channels (Austin)* **10**:320–331.

Bidaux G, Flourakis M, Thebault S, Zholos A, Beck B, Gkika D, Roudbaraki M, Bonnal JL, Mauroy B, Shuba Y, et al. (2007) Prostate cell differentiation status determines transient receptor potential melastatin member 8 channel subcellular localization and function. *J Clin Invest* **117**:1647–1657.

Bogeski I, Kummerow C, Al-Ansary D, Schwarz EC, Koehler R, Kozai D, Takahashi N, Peinelt C, Griesemer D, Bozem M, et al. (2010) Differential redox regulation of ORAI ion channels: a mechanism to tune cellular calcium signaling. *Sci Signal* **3**: ra24.

Cheang WS, Lam MY, Wong WT, Tian XY, Lau CW, Zhu Z, Yao X, and Huang Y (2013) Menthol relaxes rat aortae, mesenteric and coronary arteries by inhibiting calcium influx. *Eur J Pharmacol* **702**:79–84.

Choi S, Maleth J, Jha A, Lee KP, Kim MS, So I, Ahuja M, and Muallem S (2014) The TRPCs-STIM1-Orai interaction. *Handb Exp Pharmacol* **223**:1035–1054.

Cioffi DL (2011) Redox regulation of endothelial canonical transient receptor potential channels. *Antioxid Redox Signal* **15**:1567–1582.

Fernandez RA, Sundivakkam P, Smith KA, Zeifman AS, Drennan AR, and Yuan JX (2012) Pathogenic role of store-operated and receptor-operated Ca^{2+} channels in pulmonary arterial hypertension. *J Signal Transduct* **2012**:951497.

Fernandez RA, Wan J, Song S, Smith KA, Gu Y, Tauseef M, Tang H, Makino A, Mehta D, and Yuan JX (2015) Upregulated expression of STIM2, TRPC6, and Orai2 contributes to the transition of pulmonary arterial smooth muscle cells from a contractile to proliferative phenotype. *Am J Physiol Cell Physiol* **308**:C581–C593.

Flemming R, Xu SZ, and Beech DJ (2003) Pharmacological profile of store-operated channels in cerebral arteriolar smooth muscle cells. *Br J Pharmacol* **139**:955–965.

Genova T, Grolez GP, Camillo C, Bernardini M, Bokhobza A, Richard E, Scianna M, Lemonnier L, Valdembri D, Munaron L, et al. (2017) TRPM8 inhibits endothelial cell migration via a non-channel function by trapping the small GTPase Rap1. *J Cell Biol* **216**:2107–2130.

Hawkins BJ, Irrinki KM, Mallilankaraman K, Lien YC, Wang Y, Bhanumathy CD, Subbiah R, Ritchie MF, Soboloff J, Baba Y, et al. (2010) *S*-glutathionylation activates STIM1 and alters mitochondrial homeostasis. *J Cell Biol* **190**:391–405.

Inoue R, Jensen LJ, Shi J, Morita H, Nishida M, Honda A, and Ito Y (2006) Transient receptor potential channels in cardiovascular function and disease. *Circ Res* **99**: 119–131.

Jiao HX, Mu YP, Gui LX, Yan FR, Lin DC, Sham JS, and Lin MJ (2016) Increase in caveolae and caveolin-1 expression modulates agonist-induced contraction and store- and receptor-operated Ca^{2+} entry in pulmonary arteries of pulmonary hypertensive rats. *Vascul Pharmacol* **84**:55–66.

Johnson CD, Melanaphy D, Purse A, Stokesberry SA, Dickson P, and Zholos AV (2009) Transient receptor potential melastatin 8 channel involvement in the regulation of vascular tone. *Am J Physiol Heart Circ Physiol* **296**:H1868–H1877.

Kozai D, Ogawa N, and Mori Y (2014) Redox regulation of transient receptor potential channels. *Antioxid Redox Signal* **21**:971–986.

Kuhr FK, Smith KA, Song MY, Levitan I, and Yuan JX (2012) New mechanisms of pulmonary arterial hypertension: role of Ca^{2+} signaling. *Am J Physiol Heart Circ Physiol* **302**:H1546–H1562.

Kunichika N, Yu Y, Remillard CV, Platoshyn O, Zhang S, and Yuan JX (2004) Overexpression of TRPC1 enhances pulmonary vasoconstriction induced by capacitative Ca^{2+} entry. *Am J Physiol Lung Cell Mol Physiol* **287**:L962–L969.

Lai YC, Potoka KC, Champion HC, Mora AL, and Gladwin MT (2014) Pulmonary arterial hypertension: the clinical syndrome. *Circ Res* **115**:115–130.

Lakshmikanthan S, Zieba BJ, Ge ZD, Momotani K, Zheng X, Lund H, Artamonov MV, Maas JE, Szabo A, Zhang DX, et al. (2014) Rap1b in smooth muscle and endothelium is required for maintenance of vascular tone and normal blood pressure. *Arterioscler Thromb Vasc Biol* **34**:1486–1494.

Lashinger ES, Steiginga MS, Hieble JP, Leon LA, Gardner SD, Nagilla R, Davenport EA, Hoffman BE, Laping NJ, and Su X (2008) AMTB, a TRPM8 channel blocker: evidence in rats for activity in overactive bladder and painful bladder syndrome. *Am J Physiol Renal Physiol* **295**:F803–F810.

Lin AH, Sun H, Paudel O, Lin MJ, and Sham JS (2016) Conformation of ryanodine receptor-2 gates store-operated calcium entry in rat pulmonary arterial myocytes. *Cardiovasc Res* **111**:94–104.

Lin MJ, Leung GP, Zhang WM, Yang XR, Yip KP, Tse CM, and Sham JS (2004) Chronic hypoxia-induced upregulation of store-operated and receptor-operated Ca^{2+} channels in pulmonary arterial smooth muscle cells: a novel mechanism of hypoxic pulmonary hypertension. *Circ Res* **95**:496–505.

Liu XR, Liu Q, Chen GY, Hu Y, Sham JS, and Lin MJ (2013) Down-regulation of TRPM8 in pulmonary arteries of pulmonary hypertensive rats. *Cell Physiol Biochem* **31**:892–904.

Liu XR, Zhang MF, Yang N, Liu Q, Wang RX, Cao YN, Yang XR, Sham JS, and Lin MJ (2012) Enhanced store-operated Ca^{2+} entry and TRPC channel expression in pulmonary arteries of monocrotaline-induced pulmonary hypertensive rats. *Am J Physiol Cell Physiol* **302**:C77–C87.

Malczyk M, Veith C, Fuchs B, Hofmann K, Storch U, Schermuly RT, Witzenrath M, Ahlbrecht K, Fecher-Trost C, Flockerzi V, et al. (2013) Classical transient receptor potential channel 1 in hypoxia-induced pulmonary hypertension. *Am J Respir Crit Care Med* **188**:1451–1459.

Melanaphy D, Johnson CD, Kustov MV, Watson CA, Borysova L, Burdyga TV, and Zholos AV (2016) Ion channel mechanisms of rat tail artery contraction-relaxation by menthol involving, respectively, TRPM8 activation and L-type Ca^{2+} channel inhibition. *Am J Physiol Heart Circ Physiol* **311**:H1416–H1430.

Morrell NW, Adnot S, Archer SL, Dupuis J, Jones PL, MacLean MR, McMurtry IF, Stenmark KR, Thistlethwaite PA, Weissmann N, et al. (2009) Cellular and molecular basis of pulmonary arterial hypertension. *J Am Coll Cardiol* **54** (1 Suppl): S20–S31.

Ng LC, O'Neill KG, French D, Airey JA, Singer CA, Tian H, Shen XM, and Hume JR (2012) TRPC1 and Orai1 interact with STIM1 and mediate capacitative Ca^{2+} entry caused by acute hypoxia in mouse pulmonary arterial smooth muscle cells. *Am J Physiol Cell Physiol* **303**:C1156–C1172.

Ng LC, Ramduny D, Airey JA, Singer CA, Keller PS, Shen XM, Tian H, Valencik M, and Hume JR (2010) Orai1 interacts with STIM1 and mediates capacitative Ca^{2+} entry in mouse pulmonary arterial smooth muscle cells. *Am J Physiol Cell Physiol* **299**:C1079–C1090.

Nunes P and Demaurex N (2014) Redox regulation of store-operated Ca^{2+} entry. *Antioxid Redox Signal* **21**:915–932.

Ogawa A, Firth AL, Smith KA, Maliakal MV, and Yuan JX (2012) PDGF enhances store-operated Ca^{2+} entry by upregulating STIM1/Orai1 via activation of Akt/mTOR in human pulmonary arterial smooth muscle cells. *Am J Physiol Cell Physiol* **302**:C405–C411.

Parrau D, Ebensperger G, Herrera EA, Moraga F, Riquelme RA, Ulloa CE, Rojas RT, Silva P, Hernandez I, Ferrada J, et al. (2013) Store-operated channels in the pulmonary circulation of high- and low-altitude neonatal lambs. *Am J Physiol Lung Cell Mol Physiol* **304**:L540–L548.

Peier AM, Moqrich A, Hergarden AC, Reeve AJ, Andersson DA, Story GM, Earley TJ, Dragoni I, McIntyre P, Bevan S, et al. (2002) A TRP channel that senses cold stimuli and menthol. *Cell* **108**:705–715.

Putney JW (2009) Capacitative calcium entry: from concept to molecules. *Immunol Rev* **231**:10–22.

Remillard CV and Yuan JX (2006) TRP channels, CCE, and the pulmonary vascular smooth muscle. *Microcirculation* **13**:671–692.

Roos J, DiGregorio PJ, Yeromin AV, Ohlsen K, Lioudyno M, Zhang S, Safrina O, Kozak JA, Wagner SL, Cahalan MD, et al. (2005) STIM1, an essential and conserved component of store-operated Ca^{2+} channel function. *J Cell Biol* **169**:435–445.

Silva DF, de Almeida MM, Chaves CG, Braz AL, Gomes MA, Pinho-da-Silva L, Pesquero JL, Andrade VA, Leite MdeF, de Albuquerque JG, et al. (2015) TRPM8 channel activation induced by monoterpenoid rotundifolone underlies mesenteric artery relaxation. *PLoS One* **10**:e0143171.

Simonneau G, Gatzoulis MA, Adatia I, Celermajer D, Denton C, Ghofrani A, Gomez Sanchez MA, Krishna Kumar R, Landzberg M, Machado RF, et al. (2013) Updated clinical classification of pulmonary hypertension. *J Am Coll Cardiol* **62** (25 Suppl): D34–D41.

Smith KA, Voiriot G, Tang H, Fraidenburg DR, Song S, Yamamura H, Yamamura A, Guo Q, Wan J, Pohl NM, et al. (2015) Notch activation of Ca^{2+} signaling in the development of hypoxic pulmonary vasoconstriction and pulmonary hypertension. *Am J Respir Cell Mol Biol* **53**:355–367.

Soboloff J, Rothberg BS, Madesh M, and Gill DL (2012) STIM proteins: dynamic calcium signal transducers. *Nat Rev Mol Cell Biol* **13**:549–565.

Song MY, Makino A, and Yuan JX (2011) STIM2 contributes to enhanced store-operated Ca entry in pulmonary artery smooth muscle cells from patients with idiopathic pulmonary arterial hypertension. *Pulm Circ* **1**:84–94.

Stenmark KR, Fagan KA, and Frid MG (2006) Hypoxia-induced pulmonary vascular remodeling: cellular and molecular mechanisms. *Circ Res* **99**:675–691.

Sun J, Yang T, Wang P, Ma S, Zhu Z, Pu Y, Li L, Zhao Y, Xiong S, Liu D, et al. (2014) Activation of cold-sensing transient receptor potential melastatin subtype 8 antagonizes vasoconstriction and hypertension through attenuating RhoA/Rho kinase pathway. *Hypertension* **63**:1354–1363.

Sweeney M, Yu Y, Platoshyn O, Zhang S, McDaniel SS, and Yuan JX (2002) Inhibition of endogenous TRP1 decreases capacitative Ca^{2+} entry and attenuates pulmonary artery smooth muscle cell proliferation. *Am J Physiol Lung Cell Mol Physiol* **283**:L144–L155.

Thebault S, Lemonnier L, Bidaux G, Flourakis M, Bavencoffe A, Gordienko D, Roudbaraki M, Delcourt P, Panchin Y, Shuba Y, et al. (2005) Novel role of cold/menthol-sensitive transient receptor potential melastatine family member 8 (TRPM8) in the activation of store-operated channels in LNCaP human prostate cancer epithelial cells. *J Biol Chem* **280**:39423–39435.

Tsavaler L, Shapero MH, Morkowski S, and Laus R (2001) Trp-p8, a novel prostate-specific gene, is up-regulated in prostate cancer and other malignancies and shares

high homology with transient receptor potential calcium channel proteins. *Cancer Res* **61**:3760–3769.

Wang J, Xu C, Zheng Q, Yang K, Lai N, Wang T, Tang H, and Lu W (2017) Orai1, 2, 3 and STIM1 promote store-operated calcium entry in pulmonary arterial smooth muscle cells. *Cell Death Discov* **3**:17074.

Wang RX, He RL, Jiao HX, Dai M, Mu YP, Hu Y, Wu ZJ, Sham JS, and Lin MJ (2015) Ginsenoside Rb1 attenuates agonist-induced contractile response via inhibition of store-operated calcium entry in pulmonary arteries of normal and pulmonary hypertensive rats. *Cell Physiol Biochem* **35**:1467–1481.

Xia Y, Fu Z, Hu J, Huang C, Paudel O, Cai S, Liedtke W, and Sham JS (2013) TRPV4 channel contributes to serotonin-induced pulmonary vasoconstriction and the enhanced vascular reactivity in chronic hypoxic pulmonary hypertension. *Am J Physiol Cell Physiol* **305**:C704–C715.

Xia Y, Yang XR, Fu Z, Paudel O, Abramowitz J, Birnbaumer L, and Sham JS (2014) Classical transient receptor potential 1 and 6 contribute to hypoxic pulmonary hypertension through differential regulation of pulmonary vascular functions. *Hypertension* **63**:173–180.

Xiong S, Wang B, Lin S, Zhang H, Li Y, Wei X, Cui Y, Wei X, Lu Z, Gao P, et al. (2017) Activation of transient receptor potential melastatin subtype 8 attenuates cold-induced hypertension through ameliorating vascular mitochondrial dysfunction. *J Am Heart Assoc* **6**:e005495.

Yang XR, Lin AH, Hughes JM, Flavahan NA, Cao YN, Liedtke W, and Sham JS (2012) Upregulation of osmo-mechanosensitive TRPV4 channel facilitates chronic hypoxia-induced myogenic tone and pulmonary hypertension. *Am J Physiol Lung Cell Mol Physiol* **302**:L555–L568.

Yang XR, Lin MJ, McIntosh LS, and Sham JS (2006) Functional expression of transient receptor potential melastatin- and vanilloid-related channels in pulmonary arterial and aortic smooth muscle. *Am J Physiol Lung Cell Mol Physiol* **290**:L1267–L1276.

Yoshida T, Inoue R, Morii T, Takahashi N, Yamamoto S, Hara Y, Tominaga M, Shimizu S, Sato Y, and Mori Y (2006) Nitric oxide activates TRP channels by cysteine *S*-nitrosylation. *Nat Chem Biol* **2**:596–607.

Yu Y, Fantozzi I, Remillard CV, Landsberg JW, Kunichika N, Platoshyn O, Tigno DD, Thistlethwaite PA, Rubin LJ, and Yuan JX (2004) Enhanced expression of transient receptor potential channels in idiopathic pulmonary arterial hypertension. *Proc Natl Acad Sci USA* **101**:13861–13866.

Yu Y, Keller SH, Remillard CV, Safrina O, Nicholson A, Zhang SL, Jiang W, Vangala N, Landsberg JW, Wang JY, et al. (2009) A functional single-nucleotide polymorphism in the TRPC6 gene promoter associated with idiopathic pulmonary arterial hypertension. *Circulation* **119**:2313–2322.

Yu Y, Sweeney M, Zhang S, Platoshyn O, Landsberg J, Rothman A, and Yuan JX (2003) PDGF stimulates pulmonary vascular smooth muscle cell proliferation by upregulating TRPC6 expression. *Am J Physiol Cell Physiol* **284**:C316–C330.

Zhang S, Patel HH, Murray F, Remillard CV, Schach C, Thistlethwaite PA, Insel PA, and Yuan JX (2007) Pulmonary artery smooth muscle cells from normal subjects and IPAH patients show divergent cAMP-mediated effects on TRPC expression and capacitative Ca^{2+} entry. *Am J Physiol Lung Cell Mol Physiol* **292**:L1202–L1210.

Zhang S, Remillard CV, Fantozzi I, and Yuan JX (2004a) ATP-induced mitogenesis is mediated by cyclic AMP response element-binding protein-enhanced TRPC4 expression and activity in human pulmonary artery smooth muscle cells. *Am J Physiol Cell Physiol* **287**:C1192–C1201.

Zhang SL, Yu Y, Roos J, Kozak JA, Deerinck TJ, Ellisman MH, Stauderman KA, and Cahalan MD (2005) STIM1 is a Ca^{2+} sensor that activates CRAC channels and migrates from the Ca2+ store to the plasma membrane. *Nature* **437**:902–905.

Zhang WM, Lin MJ, and Sham JS (2004b) Endothelin-1 and IP3 induced Ca^{2+} sparks in pulmonary arterial smooth muscle cells. *J Cardiovasc Pharmacol* **44** (Suppl 1): S121–S124.

Zhang WM, Yip KP, Lin MJ, Shimoda LA, Li WH, and Sham JS (2003) ET-1 activates Ca^{2+} sparks in PASMC: local Ca^{2+} signaling between inositol trisphosphate and ryanodine receptors. *Am J Physiol Lung Cell Mol Physiol* **285**:L680–L690.

Address correspondence to: Dr. Mo-Jun Lin, Department of Physiology and Pathophysiology, School of Basic Medical Sciences, Fujian Medical University, 1 Xueyuan Road, Shangjie Zhen, Minhou County, Fuzhou, Fujian Province 350108, People's Republic of China. E-mail: mjlin@mail.fjmu.edu.cn; or Dr. James S. K. Sham, Division of Pulmonary and Critical Care Medicine, Johns Hopkins University School of Medicine, 5501 Hopkins Bayview Circle, Baltimore, MD 21204. E-mail: jsks@jhmi.edu